Hydrothermal Synthesis and Structure of a Potassium Tantalum Defect Pyrochlore

Niangao Duan,[†] Zheng-Rong Tian,[‡] William S. Willis,[‡] Steven L. Suib,*[,†,‡,§] John M. Newsam,[||] and Steven M. Levine[||]

Institute of Materials Science, University of Connecticut, Storrs, Connecticut 06269-3060, *U*-60, Charles E. Waring Laboratory, Department of Chemistry, University of Connecticut, Storrs, Connecticut 06269-4060, Department of Chemical Engineering, University of Connecticut, Storrs, Connecticut 06269-4060, and Molecular Simulations, Inc., 9685 Scranton Road, San Diego, California 92121-3752

Received January 14, 1998

The synthesis and crystal structure of potassium tantalate ($KTa_2(O,OH)_6 \cdot 1.8H_2O$) with a defect pyrochlore structure are reported. The compound was crystallized directly from tantalum pentoxide in basic solution under hydrothermal conditions at temperatures as low as 200 °C. Ion exchange of this substance in acid yielded an H-type defect pyrochlore. Both highly crystalline K-type and H-type materials absorb argon and have BET surface areas of about 14 m^2/g. The crystal structures were refined by the Rietveld least-squares method from powder X-ray diffraction data. The final R_{wp} and χ^2 were 7.70% and 2.79, respectively. The high thermal stability and control of acidity of these materials, along with the simple and cheap synthesis, may find many applications in sorption, catalysis, and microelectronics.

Introduction

Octahedral molecular sieves (OMS) have received considerable attention during the past few years given the potential applications of this new family of molecular sieves in adsorption, shape-selective catalysis, batteries, semiconductor sensors, and other areas. Instead of $(Si,Al)O_4$ tetrahedral structural units in zeolite molecular sieves, the OMS materials contain MO_6 (M = metal) octahedra as the basic building block in forming three-dimensional porous framework structures.[1] Typical octahedral molecular sieves are the oxides of early transition metals, such as Mo,[2] Ti,[3,4] and Mn,[5] and consist of either pillared octahedral layered materials or three-dimensional octahedral tunnel structures.

Potassium tantalum pyrochlore, $KTa_2(O,OH)_6 \cdot 1.8H_2O$, is another porous octahedral molecular sieve with three-dimensional tunnels. The pyrochlore structure can be viewed as having an M_2O_6 framework composed exclusively of vertex-shared octahedra. The framework is permeated by tunnels with cavities of tetrahedral symmetry occurring at tunnel intersections. The ideal structure is cubic with space group $Fd\bar{3}m$ and eight formula units per unit cell. The general formula for a stoichiometric pyrochlore[6] is $A_2M_2O_6O'$. The O′, A, and M ions occupy special positions 8*b*, 16*d*, and 16*c*, respectively. The remaining O occupies the 48*f* position. The defect pyrochlore structure[7−11] with formulas $A_2M_2O_6$, retains the same 3-D framework, except that the A ions are in 8*b* positions or general 32*e* positions. In both defect and normal pyrochlore materials, the A ions, positioned in the cavity, can be readily ion exchanged, a property characteristic of zeolites.

Pyrochlore type materials are generally used as fast ion conductors and in screen printing resistors.[6,12−16] They are often prepared by solid state methods at high temperature (ca. 1200 °C). Hydrothermal syntheses of stoichiometric calcium niobium and tantalum pyrochlores using alkoxides as starting materials were reported recently.[17] In the present work, potassium tantalates with the defect pyrochlore structure were crystallized directly from tantalum pentoxide in basic solutions at 200 °C. Rietveld analysis of X-ray powder diffraction data was employed to refine the structure, and various other analytical methods were used to characterize this octahedral molecular sieve. The direct

* To whom correspondence should be addressed.
[†] Institute of Materials Science, University of Connecticut.
[‡] *U*-60, Charles E. Waring Laboratory, Department of Chemistry, University of Connecticut.
[§] Department of Chemical Engineering, University of Connecticut.
[||] Molecular Simulations, Inc.

(1) Wells, A. F. *Structural Inorganic Chemistry*; 5th ed.; Clarendon Press: Oxford: 1985.
(2) Lalik, E.; Kolodziejski, W.; Lerf, A.; Klinowski, J. *J. Phys. Chem.* **1993**, *97*, 223−229.
(3) Watanabe, M.; Fujiki, Y. *J. Solid State Chem.* **1987**, *66*, 56−63.
(4) Anderson, M. W.; Klinowski, J. *J. Inorg. Chem.* **1990**, *29*, 3260−3263.
(5) Suib, S. L. In *Recent advances and New Horizons in Zeolite Science and Technology*; Chon, H., Woo, S. I., Park, S. E., Eds.; Elsevier: Amsterdam, 1996; Vol. 102, pp 47−74.
(6) Subramanian, M. A.; Aravamudan, G.; Subba Rao, G. V. *Prog. Solid State Chem.* **1983**, *15*, 55.
(7) Ganne, M.; Tournoux, M. *Mater. Res. Bull.* **1975**, *10*, 1313−1318.
(8) Groult, G.; Pannetier, J.; Raveau, B. *J. Solid State Chem.* **1982**, *41*, 277−285.
(9) Murphy, D. W.; Dye, J. L.; Zahurak, S. M. *Inorg. Chem.* **1983**, *22*, 3679−3681.
(10) Murphy, D. W.; Cava, R. J.; Rhyne, K.; Roth, R. S.; Santoro, A.; Zahurk, S. M.; Dye, J. L. *Solid State Ionics* **1986**, *18* and *19*, 799−801.
(11) Isasi, J.; Lopez, M. L.; Veiga, M. L.; Pico, C. *Solid State Ionics* **1996**, *89*, 321−326.
(12) Jona, F.; Shirane, G.; Pepinsky, R. *Phys. Rev.* **1955**, *98*, 903−909.
(13) Goodenough, J. B.; Hong, H. Y.-P.; Kafalas, J. A. *Mater. Res. Bull.* **1976**, *11*, 203−220.
(14) Lukaszewicz, K.; Pietraszko, A.; Stepien-Damm, J. *Mater. Res. Bull.* **1994**, *29*.
(15) Heremans, C.; Wuensch, B.; Stalick, J.; Prince, E. *J. Solid State Chem.* **1995**, *117*, 108−121.
(16) Thomson, J. B.; Armstrong, A. R.; Bruce, P., G. *J. Am. Chem. Soc.* **1996**, *118*, 11129−11133.
(17) Lewandowski, J. T.; Pickering, I. J.; Jacobson, A. J. *Mater. Res. Bull.* **1992**, *27*, 981−988.

S0020-1669(98)00040-8 CCC: $15.00
Published on Web 08/20/1998

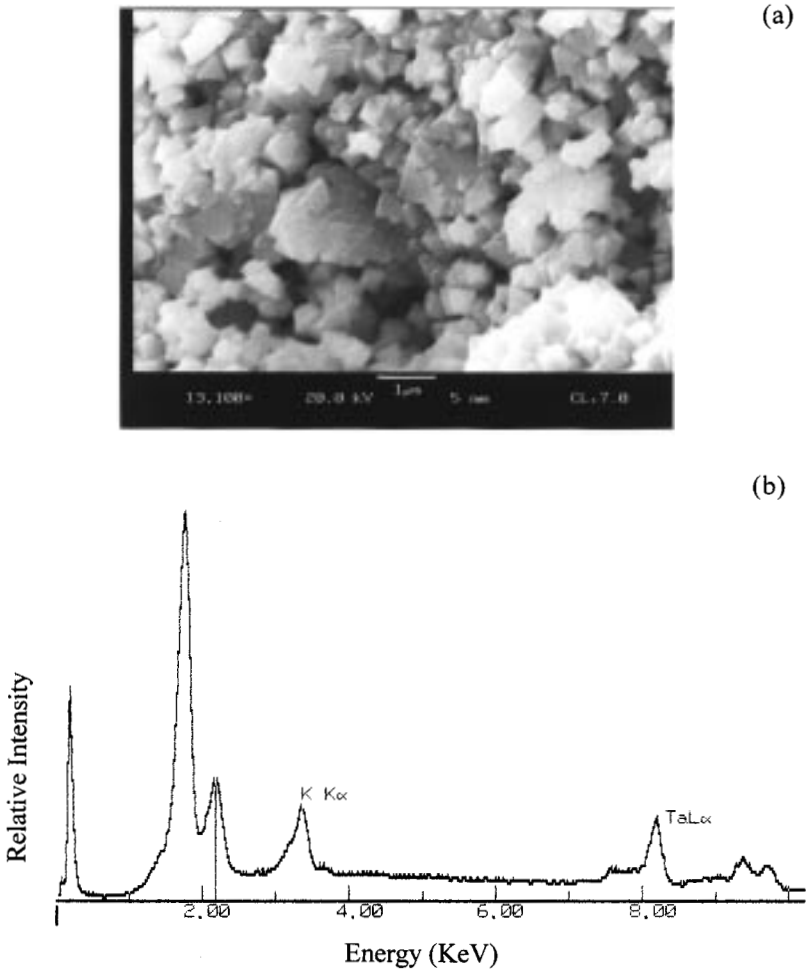

Figure 1. (a) Scanning electron micrographs showing different morphologies of the individual crystals. (b) Energy dispersive X-ray spectra for atoms K and Ta and their relative concentrations.

transformation to a pyrochlore from crystalline tantalum oxide may pose questions regarding the growth mechanism, which may provide insight for further synthetic efforts.

Experimental Section

Sample Preparation. The title compound is prepared as follows: 21 g of potassium hydroxide was dissolved in 75 mL of deionized distilled water (DDW) at room temperature. The solution was combined with 3 g of tantalum pentoxide with magnetic stirring. The resulting slurry was loaded into a 90-mL Teflon-lined digestion autoclave. The autoclave was then sealed and heated to 200 °C in an oven for 2 days. The solid product was washed with DDW in a centrifuge a few times and air-dried. To obtain the H-form of the material by ion exchange, 0.5 g of as-synthesized solid was added to 100 mL of 5 N HNO_3 and stirred at 40 °C for 24 h. The product was recovered by centrifuge separation and washed with an excess of DDW.

Characterization. X-ray diffraction data were collected using a Scintag XDS 2000 diffractometer with Cu Kα radiation. The samples were slowly ground in an agate mortar under acetone to ensure a particle size smaller than 10 μm and loaded into a side-packed sample holder to minimize preferred orientation.[18] The divergence and receiving slits used were 1 mm and 0.3 mm, and the scattering slits for the X-ray tube and detector sides were 2 mm and 0.5 mm, respectively. Data were collected between 8° and 100° in 2θ, with a step size of 0.01°, and a count time of 4 s/step.

The powder pattern indexing and lattice parameter refinement were performed by TREOR 90 through the Cerius^2 interface.[19] The Rietveld analysis[19,20] of the powder X-ray data was carried out using the GSAS program[21−26] through Materials Science Simulation of MSI. Trial structures were developed and visualized using the InsightII and Cerius^2 crystallographic modeling package.

Scanning electron microscopy was performed on an Amray 1645 scanning electron microscope using conventional sample preparation and imaging techniques. Chemical compositions were determined by energy dispersive X-ray analysis in a Philips PV9800 EDAX spectrometer with the Super Quant program. Elemental analyses for K and Ta were determined by inductively coupled plasma (ICP) analysis with a Jarrel Ash 975 instrument.

Differential scanning calorimetry (DSC) and thermogravimetric analyses (TGA) were carried out with DuPont DSC 910 and DuPont 951 TGA systems, respectively. About 5 mg of sample powder was loaded into an aluminum sample pan with a cover for DSC and a

(18) McMurdie, H. F.; Morris, M. C.; Evans, E. H.; Paretzkin, B.; Wong-Ng, W. *Powder Diffr.* **1986**, *1*, 40−43.

(19) *InsightII and Cerius2 crystallographic modeling package*; Molecular Simulations Inc.: San Diego, CA, 1996.

(20) Rietveld, H. M. *J. Appl. Crystallogr.* **1969**, *2*, 65−71.

(21) Larson, A. C.; Von Dreele, R. B. *GSAS Generalized Structure Analysis System*; Los Alamos National Laboratory: Los Alamos, NM, 1994.

(22) Rotella, F. J.; Jorgensen, J. D.; Morosin, B.; Biefeld, R. M. *Solid State Ionics* **1981**, *5*, 455−458.

(23) Slade, R. C. T.; Hall, G. P.; Ramanan, A.; Prince, E. *Solid State Ionics* **1996**, *92*, 171−181.

(24) Thompson, P.; Cox, D. E.; Hastings, J. B. *J. Appl. Crystallogr.* **1987**, *20*, 79−83.

(25) Suortti, P. *J. Appl. Crystallogr.* **1972**, *5*, 325−331.

(26) Jacobson, A. J.; Lewandowski, J. T.; Mims, C. A.; Hall, R. B.; Meyers, G. R. In *Chemistry of Electronic Ceramic Materials*; Davies, P. K., Roth, R. S. Eds.; NIST Special Publication 804; NIST: Gaithersburg, MD, 1991.

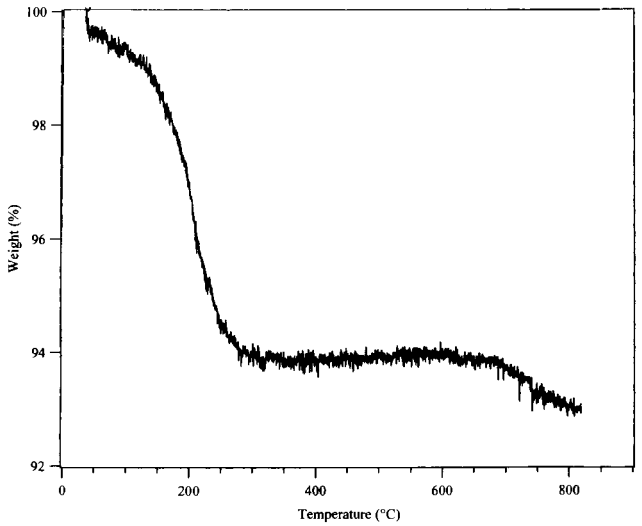

Figure 2. Thermogravimetric analysis of $KTa_2(O,OH)_6 \cdot 1.8H_2O$ materials in a N_2 atmosphere.

platinum sample holder for TGA. Both nitrogen and oxygen gases were used as carrier gases for TGA experiments to check oxygen loss during heating. The flow rates of both gases are about 30 mL/min.

A Nicolet Magna-IR 750 spectrometer was used to perform Fourier transform infrared experiments via diffuse reflectance methods. The data were collected at room temperature, 150 °C, and 250 °C.

Adsorption data were obtained on a Cahn microbalance Model C 2000 system. The calcined samples were dehydrated by outgassing under vacuum above 10^{-5} Torr on increasing temperatures up to 300 °C until constant weight was obtained. Research grade argon was used for physisorption measurements at 300 °C. A typical run consisted of adsorption up to 760 Torr, and then a desorption cycle was carried out to ensure equilibrium at each pressure. For the argon adsorption, the saturated pressure (P_0) was taken as 1.82 atm as supercooled liquid at 195 K. A molecular cross-sectional area of 16.2 Å^2 was used for BET surface area calculations.

Results

Indexing of the X-ray diffraction pattern and least-squares refinement based on the crucial peak positions yields a cubic unit cell with $a_0 = 10.6193(3)$ Å. The sharpness of the diffraction indicates that the as-synthesized material is highly crystalline. In confirmation, scanning electron microscopy (Figure 1) reveals various crystal habits such as cubes, octahedra, and plates with uniform crystal sizes of about 0.5 μm. Energy dispersive X-ray analyses on the octahedral surfaces of the individual crystals under the SEM gave an average K:Ta ratio of 0.6:1, close to the ratio of 0.52:1, obtained by inductively coupled plasma elemental analyses.

Thermogravimetric analyses (Figure 2) indicate a 1% weight loss below 160 °C, and a 6.5% weight loss beginning at 200 °C. A further weight change occurs around 750 °C; X-ray diffraction patterns of the sample calcined above this temperature show a collapse of the pyrochlore structure.

The Fourier transform infrared spectra collected at different temperatures by the diffuse reflectance method are shown in Figure 3. The broad bands around 3300 cm^{-1} indicate the presence of O−H stretches from water molecules in the crystal structure. The band intensities are gradually decreased on removal of water from the pyrochlore by in situ heating in two stages from room temperature to 160 °C to 250 °C. The sharp absorption peaks around 3600 cm^{-1} are characteristic of free hydroxyl group stretches in the framework lattice.

This material readily undergoes ion exchange in a 5 M nitric acid solution at 40 °C. After 12 h, the potassium in the material

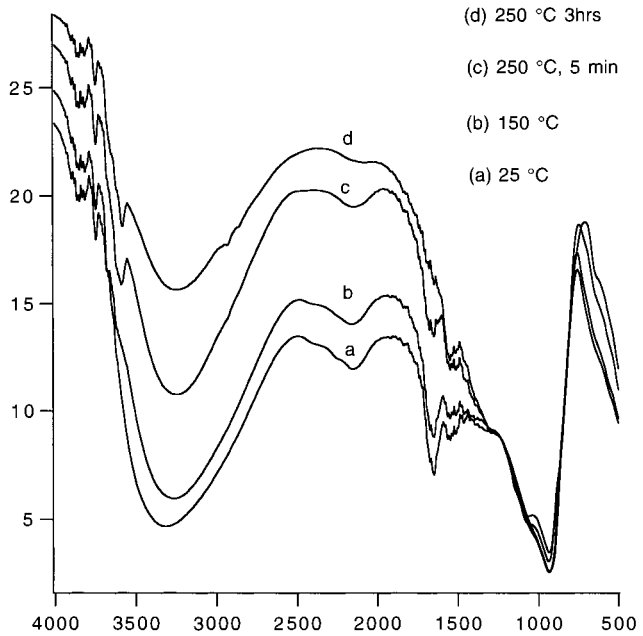

Figure 3. Diffuse reflectance FTIR spectra of $KTa_2(O,OH)_6 \cdot 1.8H_2O$ at different temperatures: (a) room temperature, (b) 150 °C, (c) 250 °C after 5 min, and (d) 250 °C after 3 h.

Table 1. $KTa_2(O,OH)_6$ Overall Refinement Information[a]

unit cell setting	cubic
space group	$Fd\bar{3}m$
data collection temp (K)	295
a (Å)	10.619 28(31)
unit cell volume (Å^3)	1197.53(6)
unit cell contents	KTa_2O_5OH
empirical formula	$K_{0.52}Ta_2O_5OH \cdot 1.8H_2O$
profile R-factor (R_p)	0.0531
weighted profile R-factor (R_{wp})	0.0770
reduced χ^2	2.790
min d-space refln (Å)	0.8155(2)
max d-space refln (Å)	6.1312(2)
no. of unique X-ray reflns	46

[a] Rietveld refinement was used to minimize $\sum w_i(I_{o,i} - I_{c,i})^2$, where $I_{o,i}$ and $I_{c,i}$ are the observed and calculated powder diffraction intensities for the ith point, respectively. Weighted and unweighted profile R-factors are defined as $R_{wp} = \{[\sum w_i(I_{o,i} - I_{c,i})^2]/[\sum w_i(I_{o,i})^2]\}^{1/2}$ and $R_p = \sum|I_{o,i} - I_{c,i}|/\sum I_{o,i}$. The expected R-factor (the statistically best possible value for R_{wp}) is defined as $R_e = [(N - P)/\sum w_i(I_{o,i})^2]^{1/2}$, where N is the number of observed powder diffraction data points and P is the number of parameters refined.

is completely exchanged by H^+, as evidenced by EDX analysis in the SEM: no detectable potassium X-ray spectrum was observed. The BET surface area measurements for the K^+- and H^+-form pyrochlore are 13.5 and 10.5 m^2/g, respectively. After heating at 400 °C in a vacuum, the BET surface area of the K^+ form decreased to 5 m^2/g.

The crystal structure refinement was undertaken by Rietveld analysis of the powder X-ray diffraction data. The defect pyrochlore structure, $Tl_2Ta_2O_6$,[7] was used as the initial model with space group $Fd\bar{3}m$. The (111) reflection at $2\theta = 14.43°$ was excluded from the refinement because of its asymmetry and sensitivity to experimental artifacts. No attempt was made to locate proton positions. The details of the refinement parameters are summarized in Tables 1 and 2. The resulting atomic positions and isotropic temperature factors and selected interatomic distances are listed in Tables 3 and 4, respectively. Final observed, calculated, and difference X-ray powder-diffraction patterns are plotted in Figure 4.

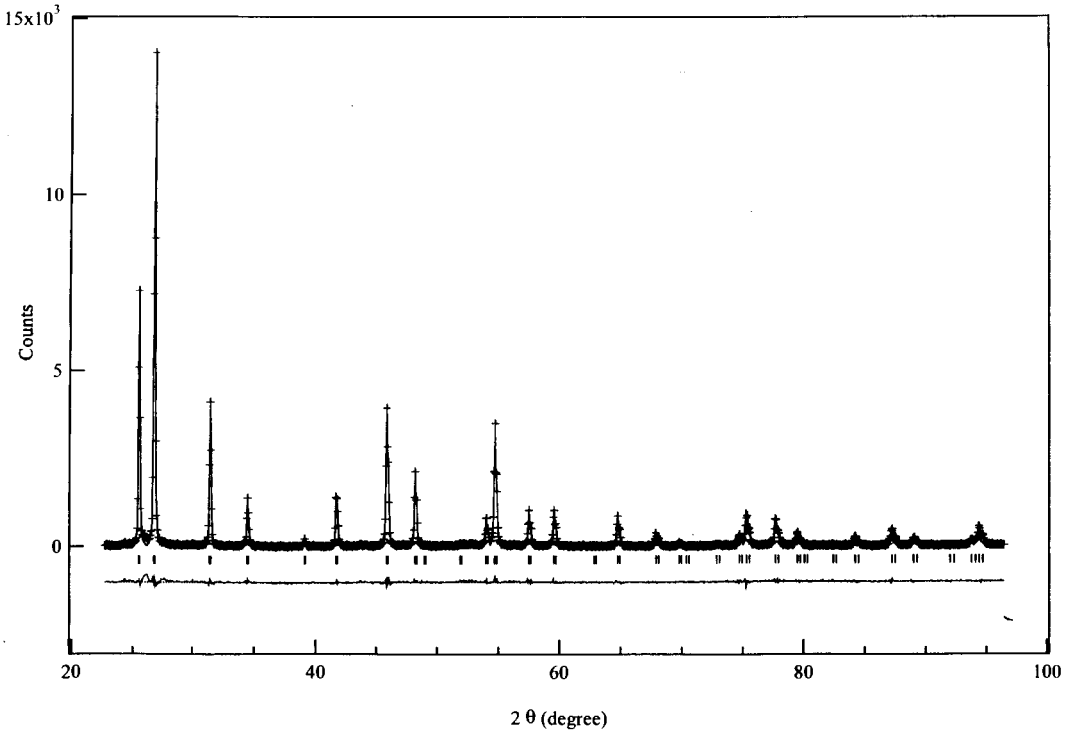

Figure 4. The observed (+), calculated (solid line), and difference (bottom curve) powder X-ray diffraction profiles for $KTa_2(O,OH)_6 \cdot 1.8H_2O$.

Table 2. Individual Diffractogram Information[a]

profile *R*-factor (R_p)	0.0531
weighted profile *R*-factor (R_{wp})	0.0770
expected profile *R*-factor (R_E)	0.054
wavelength (Å)	1.5406
min 2 θ (deg)	12.00
max 2 θ (deg)	100.00
max d-space refln (Å)	6.1312(2)
no. of reflns	48
zero correction (deg)	−0.0078
abs correction[b]	A_{b1}, 0.70, A_{b2}, 0.036
profile params[c]	pseudo-Voigt with asym correction
U, *V*, *W* (deg^2)	7.7, −11.1, 8.8
asym correction	0.0038
X, *Y*, *P*	1.82(1), 13.65(2), 3.77(1)
background function[d]	10 coefficient Chebyshev polynomial

[a] Rietveld refinement was used to minimize $\sum w_i(I_{o,i} - I_{c,i})^2$, where $I_{o,i}$ and $I_{c,i}$ are the observed and calculated powder diffraction intensities for the ith point, respectively. Weighted and unweighted profile *R*-factors are defined as $R_{wp} = \{[\sum w_i(I_{o,i} - I_{c,i})^2]/[\sum w_i(I_{o,i})^2]\}^{1/2}$ and $R_p = \sum|I_{o,i} - I_{c,i}|/\sum I_{o,i}$. The expected *R*-factor (the statistically best possible value for R_{wp}) is defined as $R_e = [(N - P)/\sum w_i(I_{o,i})^2]^{1/2}$ where *N* is the number of observed powder diffraction data points and *P* is the number of parameters refined. The Bragg *R*-factor, R_B, is defined as $R_B = \sum|F_o^2 - F_c^2|/\sum F_o^2$ using estimated values for the observed structure factors, F_o. [b] Reference 25. [c] Reference 24. [d] Reference 21.

Table 3. Atomic Parameters for $KTa_2(O,OH)_6$ Defect Pyrochlore

atom	site	*x*	*y*	*z*	U_{iso}	fractional
Ta	16*c*	0	0	0	0.0105(3)	1
K	16*d*	0.5	0.5	0.5	0.0176(3)	0.532(11)
O1	48*f*	0.3138(4)	0.125	0.125	0.0004(15)	1
O2	32*e*	0.4351(12)	0.4351(12)	0.4351(12)	0.0744(19)	0.429(40)

Discussion

A. Composition. The precursor to this potassium tantalate pyrochlore is crystalline Ta_2O_5 in an excess of KOH solution. Elemental analysis for K and Ta in the product gave a K:Ta ratio of 0.52:1.00. Assuming that the oxidation state of tantalum is 5+, the chemical formula can be written as $K_{0.52}TaO_{2.76}$ or $K_{1.04}Ta_2O_5$. For pyrochlore structures, there exist two chemical formulas, an ideal structure of $A_2M_2O_7$ and a defect structure of $A_2M_2O_6$. Clearly, the synthesized material is closer to the defect structure composition. To maintain charge balance, one of the oxygens in the M_2O_6 moiety must be replaced by an OH (hydroxyl group), the presence of which is manifested by the bands at ~3600 cm^{-1} in the FTIR spectra (Figure 3). Rietveld structural analysis gave an occupancy number of K of 0.532(11), close to the ICP elemental analysis data. The thermogravimetric data indicate a total weight loss of 6.1% up to 750 °C (Figure 2). Using the formula $K_{1.04}Ta_2O_5OH \cdot xH_2O$ for the K^+ form, this corresponds to some 1.8 water molecules per unit cell, a value confirmed by the water occupancy obtained in the Rietveld refinements (see discussion in crystal structural section). Therefore, we conclude that the chemical formula of this material is $KTa_2O_5OH \cdot 1.8H_2O$.

Table 4. Framework Interatomic Distances and Angles

Distances (Å)			
Ta−O(1)		1.9959(15)	
K−O(1)		2.7262(31)	
K−O(2)		2.863(14)	
Angles (deg)			
O(1)−Ta−O(1)	90.54(16)	O(1)−K−O(1)	117.975(30)
O(1)−Ta−O(1)	89.46(16)	O(1)−K−O(1)	179.980(0)
Ta−O(1)−Ta	140.29(23)	O(1)−K−O(1)	62.025(30)

B. Crystal Structure. The structure of $KTa_2O_5OH \cdot 1.8H_2O$ is a defect pyrochlore. Neutron powder diffraction studies of H-type structures have already been reported[8,22,23] with particular interest focusing on the proton positions. In this work, a single-crystal diffraction study of $Tl_2Ta_2O_6$ was chosen as the starting model, and the structure was refined in space group $Fd\bar{3}m$ (origin of point symmetry 3*m*; second choice). After scale factor and background refinement, the zero point and lattice parameter were optimized. A pseudo-Voigt peak shape function was used,[24] with the half-width parameters *U*, *V*, *W*, and an asymmetry correction initially kept constant. For an ideal sample these parameters are instrumental characteristics, mea-

sured by fitting data for a Standard Reference Material for line broadening in powder X-ray diffraction. The shape profile was fitted after *X*, *Y*, shift, and *P* were refined.[24]

The Ta atoms adopt the 16*c* sites while the O atoms occupy the 48*f* position as in most defect pyrochlores. The refined oxygen *x* coordinate 0.3138(4) is in good agreement with literature results for both powder and single-crystal diffraction data.[7,17] About one-fifth of the oxygen atoms occurs as hydroxyl groups, which are apparently randomly distributed over these sites. The K atoms adopt the 16*d* sites, and refinement gives an occupy factor of 0.532(1). Allowing the K^+ occupancy to vary lowered the *R* value significantly.

The 32*e* sites were also considered for K atoms, but although nonzero occupancies of up to 0.27 were found, there was no significant *R*-factor improvement and a K^+ 32*e* site had a negative thermal parameter. Therefore, this position for K was eliminated. Water molecules are indicated to be located in the tunnels by the TGA and FTIR results. The water oxygen atoms are taken to occupy the 32*e* general position. Refinement of position and occupancy factors of this site resulted in a decrease in the *R* value and χ^2. The fractional occupancy corresponds to 1.7 water molecules per unit cell ($f = 0.43(4)$), close to the value of 1.8 obtained from the TGA experiments.

The refinement of isotropic thermal parameters yields a negative value for oxygen atoms at 48*f* site. This may be caused by the surface roughness of the sample, which can strongly reduce the intensity of Bragg reflections at low scattering angles.[21] It is even more severe for a sample with high absorption such as tantalum oxide. A Suortti[25] function in GSAS is employed to refine the powder absorption effect. Reasonable temperature factors are obtained thereafter.

The bond lengths and bond angles, listed in Table 4, are in good agreement with the single-crystal X-ray diffraction data.[7] The final R_{wp}, R_p, and χ^2 are 7.70%, 5.31%, and 2.79, respectively.

C. Sorption, Ion Exchange Properties, and Thermal Stability. Various crystal morphologies are observed in the SEM micrographs. The crystal sizes are between 0.3 and 1 μm, and no amorphous components are evident. The material density is 5.845 g/cm^3. Using 1 μm as a radius for the nonporous spherical particles, the external surface area is calculated to be about 0.5 m^2/g. The BET surface area of 14 m^2/g of this defect pyrochlore suggests that there is considerable internal surface adsorption.

The porous nature of this material is further evidenced by the fast ion exchange in acid solution. The H-form of this defect pyrochlore has a surface area of 12.5 m^2/g, close to that of the parent K-type of materials. Heating to 450 °C in a vacuum caused a decrease of BET surface area to about 5 m^2/g, indicating a partial structural change at this temperature.

At ambient pressure, the materials start to lose water around 200 °C, which could be attributed to water bound in the cavities. In the FTIR spectra, the water absorption bands (3300 cm^{-1}) decreased when samples were heated to 250 °C. This provides strong support for loss of water up to 250 °C. At 750 °C, onset of an additional weight loss indicates oxygen evolution from the framework; X-ray diffraction data indicate a phase transformation to a perovskite related phase.[26]

Finally, regarding catalytic properties, this defect pyrochlore is expected to show strong acidity similar to hydrated tantalum oxides.[27] Compared to other acid catalysts, such as zeolites which are normally stable up to 600 °C, the tantalum oxide OMS systems may have much better thermal stability. Along with the three-dimensional pore structure, they may find potential applications in high-temperature combustion and other related catalytic processes.

Conclusions

In the present study, potassium tantalate with the defect pyrochlore structure has been successfully prepared by hydrothermal alteration methods and characterized by several techniques, including crystal structure determination by Rietveld refinement of in-house powder X-ray diffraction data. Thermal analyses indicate thermal stability up to 900 °C. The small pore microporosity and ion exchange capacity were verified by BET surface area measurements and by ion exchange in nitric acid. The combination of reasonable surface area, microporosity, ion exchange capacity, and acidity that this material shows suggests potential catalytic and adsorption applications. The present work also illustrates that crystalline Ta_2O_5 has at least partial solubility in basic solutions under hydrothermal conditions, suggesting that other tantalum oxide octahedral molecular sieves might be accessible.

Acknowledgment. We thank the Department of Energy, Office of Basic Energy Sciences, Division of Chemical Sciences, and Molecular Simulations, Inc. for support of this research. N.D. acknowledges Drs. James Knox, Amado Garcia-Ruitz, and Stephanie Brock for helpful discussions and technical assistance.

IC980040S

(27) Ushikubo, T.; Wada, K. *Appl. Catal.* **1990**, *67*, 25−38.